JOC The Journal of Organic Chemistry

Article

pubs.acs.org/joc

How Microsolvation Numbers at Li Control Aggregation Modes, sp^2-Stereoinversion, and NMR Coupling Constants $^2J_{H,H}$ of $H_2C{=}C$ in α-(2,6-Dimethylphenyl)vinyllithium

Rudolf Knorr,* Claudia Behringer, Ernst Lattke, Ulrich von Roman, and Monika Knittl

Department Chemie, Ludwig-Maximilians-Universität München, Butenandtstrasse 5-13 (Haus F), 81377 München, Germany

Supporting Information

ABSTRACT: The title compound **4** is a trisolvated monomer **4**&3THF in THF solution and dimerizes *endo*thermically to form (**4**&THF)$_2$ with a strongly positive (!) dimerization entropy in toluene as the solvent. In the absence of electron-pair donor ligands, **4** aggregates (>dimer) in hydrocarbon solutions. These results followed from the ^{13}C-α splitting patterns and the magnitudes of the one-bond ^{13}C,^{6}Li NMR coupling constants in combination with lithiation NMR shifts as secondary NMR criteria. The rate constants of cis/trans sp^2-stereoinversion could be measured on the ^{1}H NMR time scale in THF, in which solvent the preinversion lifetime is 0.24 s at 25 °C. This inversion proceeds according to the pseudomonomolecular, ionic mechanism with the typical, strongly negative pseudoactivation entropy. In a different mechanism, the lifetimes are much longer at 25 °C for the dimer (**4**&*t*-BuOMe)$_2$ in toluene (ca. 2.5 min) and for donor-free, aggregated **4** in hexane solution (roughly 1 min). The olefinic interproton two-bond coupling constants $^2J_{H,H}$ of the $H_2C{=}CLi$ part are proposed as an indicator of microsolvation at Li, because they were found to increase linearly with the "explicit" solvation of α-arylvinyllithiums by 0, 1, 2, and 3 electron-pair donor ligands.

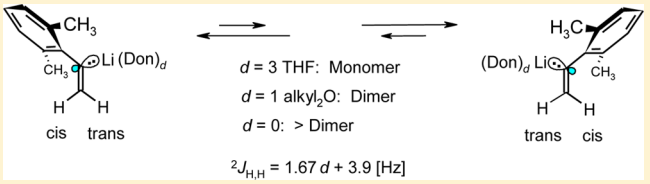

INTRODUCTION

Microsolvation numbers *d* count the electron-pair donor ligands ("Don" in Scheme 1) that are coordinated to a cation such as Li^+ in its first solvation shell. Except for rare examples,[1−3] such *d* values of carbanionic lithium compounds in coordinating solvents[4−6] usually could not be determined precisely from NMR spectra if the usual rapid scrambling of coordinated and free ligands led to averaged NMR signals even at very low temperatures. More recently, such scrambling was found[7−9] to be sufficiently retarded also in a family of sterically congested alkenyllithiums **1**, which displayed separately integratable ^{1}H and ^{13}C NMR signals of coordinated and free monodentate (but nonchelating) ligands of the ethereal type alkyl$_2$O. This straight evidence of microsolvation numbers turned out to be connected with the scalar NMR coupling constant $^1J_{C,Li}$ between ^{13}C-α (Scheme 1) and directly bound lithium nuclei, as formulated in the empirical eq 1 that proved[7] to be valid for simple alkyl-, alkenyl-, phenyl-, and alkinyllithiums whose microsolvation numbers cannot (yet?) be determined in this direct manner.[10] The connectivity numbers *n* and *a* in eq 1 are defined as follows: *n* is the number of lithium cations in contact with a certain carbanionic center C-α under consideration, while *a* specifies how many C-α centers are coordinated to a certain Li cation.[11] The sensitivity factors *L* in eq 1 depend on the organolithium constitution[10] and have almost equal values for the monomers and dimers of alkenyllithiums **1**−**3**: *L* = 42.8 Hz for **1a**,**b**[7] and for a truncated version[9] of **1**; 42.0 Hz[12] for **2**; 44.5 Hz[13] for **3**. The simple tool of eq 1 hinges on knowing (or guessing) the value of *L*, whose determination requires measuring the $^1J_{C,Li}$ magnitude of at least one organolithium species with a known (or obvious) aggregational state and microsolvation number *d*. Other recently advanced NMR techniques utilize diffusion-ordered spectroscopy (DOSY)[14,15] or the methods of continuous variation[16] (MCV, or Job plots).

$$d = L \times (n \times {}^1J_{C,Li})^{-1} - a \quad (1)$$

Equation 1 remains applicable under conditions of the above-mentioned rapid ligand scrambling as long as intermolecular

Scheme 1. Constitutions of Previously (1−3) and Presently (4, 5) Studied Alkenyllithiums

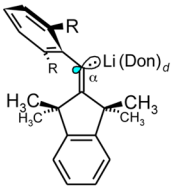

1

1	R
a	H
b	CH_3

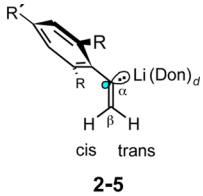

2-5

2-5	R	R´
2	$C(CH_3)_3$	H
3	$CH(CH_3)_2$	H
4	CH_3	H
5	CH_3	CH_3

Received: April 7, 2015
Published: June 1, 2015

DOI: 10.1021/acs.joc.5b00762
J. Org. Chem. 2015, 80, 6313−6322

scrambling of the Li cations does not destroy the $^{13}C/^{6}Li$ spin–spin coherence that provides the $^{1}J_{C,Li}$ values (usually only at sufficiently low temperatures). The ^{6}Li isotope is commonly employed since it gives simpler and better resolved ^{13}C-α resonances[17] than the more abundant isotope ^{7}Li. With the nuclear spin quantum number of $I = 1$ for ^{6}Li, the $^{13}C,^{6}Li$ coupling constant splits the ^{13}C-α resonance into $2nI + 1 = 2n + 1$ components as follows: A triplet of three equally intense signals (1:1:1) for the CLi_1 part of a monomer ($n = a = 1$); a 1:2:3:2:1 quintet for the CLi_2 moieties of a dimer or a cyclooligomer ($n = a = 2$); a 1:3:6:7:6:3:1 septet for the CLi_3 motifs in a tetramer (where $n = a = 3$).[4,11] These splitting patterns (whose frequency intervals equal $^{1}J_{C,Li}$) provide reliable evidence of the aggregational state, unless a coordinatable heteroatom within an organolithium compound might cause higher aggregation than indicated by the above signal multiplicities. In this way, it was shown[12] that two *tert*-butyl (*t*-Bu) substituents in the *ortho* positions caused **2** to be entirely monomeric in THF, Et_2O, or *tert*-butyl methyl ether (*t*-BuOMe) as the solvent, whereas the *o*-/*o*′-diisopropyl groups in **3** admitted dimerization:[13] **3** turned out to be monomeric in THF and was mainly dimeric in *t*-BuOMe, whereas it was a monomer/dimer mixture in Et_2O. These two β-unsubstituted α-arylvinyllithiums (**2** and **3**) served as test objects for eq 1 since some of their microsolvation numbers *d* were confirmed through NMR integration of separated NMR signals of the following coordinated ligands: *N*,*N*,*N*′,*N*′-tetramethyl-1,2-diaminoethane (TMEDA, 1 equiv, $d = 2$ per Li)[12] with monomeric **2** in *t*-BuOMe (at ≤ -68 °C) or in toluene (at ≤ -44 °C) as the solvents, and the coordinated portion (1 equiv)[13] of the solvent *t*-BuOMe ($d = 1$ per Li) with dimeric **3** at ≤ -69 °C. On this basis, we will use the magnitude of $^{1}J_{C,Li}$ in eq 1 as the remaining primary criterion for those alkenyllithiums that are no longer able to offer separately integratable NMR signals of free and immoblized portions of a donor ligand. As such a case, the title compound **4** will be presented here as the first one of our β-unsubstituted vinyllithiums that occurs in more than two species with different degrees of aggregation and microsolvation. In particular, **4** will serve also for the purpose of developing secondary criteria of microsolvation.

RESULTS AND DISCUSSION

A. Donor-Solvated Monomers and Dimers of α-(2,6-Dimethylphenyl)vinyllithium (4). The preparation (Scheme 2) of the title compound **4** through Br/Li interchange of the known[18] α-bromoalkene **6** in Et_2O or *t*-BuOMe with *n*-butyllithium (*n*-BuLi) in hexane or cyclopentane was already described.[19] However, this method was unprofitable in THF as the solvent[20] since **4** coupled quickly with its coproduct 1-bromobutane (*n*-BuBr) to give **8** and LiBr. In a side-reaction that occurred in almost any solvent, either **4** or surplus *n*-BuLi eliminated HBr from α-bromoalkene **6** with formation of LiBr and the alkene **9**[19] (this only from **4**) along with the alkyne intermediate that consumed a further organolithium equivalent to generate the lithium acetylide **10**. Crystallization and purification[19] separated **4** from such contaminations and afforded single crystals of the disolvated dimers $(\mathbf{4}\&Et_2O)_2$ or $(\mathbf{4}\&t\text{-BuOMe})_2$.

In THF as the solvent (Figures S1–S3, Supporting Information),[21] the above two kinds of crystalline, disolvated dimers of **4** deaggregated with complete replacement of their original donor ligands by solvent molecules to form monomeric

Scheme 2. Preparation, Derivatives, and π Orbital Arrangement (7) of the Title Compound 4

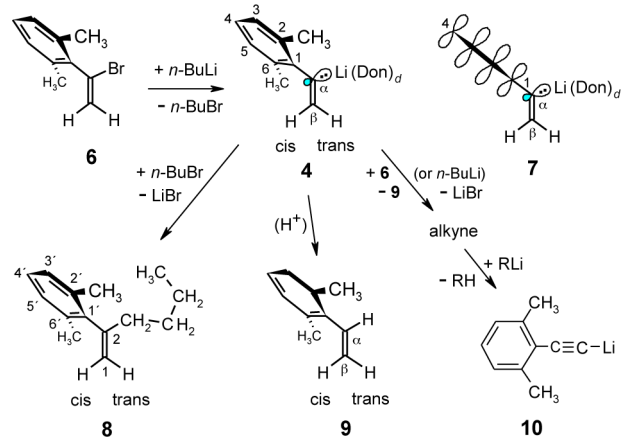

4&3THF. This became evident by means of the two primary diagnostic tools that were explained in the Introduction: First, detection of a triplet (1:1:1) splitting pattern of ^{13}C-α in $[^{6}Li]\mathbf{4}$ at and below −58 °C established the CLi_1 part of a monomer (hence, $n = a = 1$), whereas the quintet pattern (1:2:3:2:1) reported earlier[19] for *t*-BuOMe-solvated **4** in toluene at and below −35 °C had established the CLi_2 motif of a dimer ($n = a = 2$). Second, the magnitudes of $^{1}J_{C,Li} = 11.6$ Hz for the monomer and 7.5 Hz[19] for the dimer are simultaneously compatible with a common sensitivity factor of $L = 46$ (±1) Hz in the empirical[7] eq 1: Within the error limits of the two $^{1}J_{C,Li}$ values, eq 1 disclosed the monomer to be microsolvated by $d = 3$ THF and the dimer by $d = 1$ *t*-BuOMe ligand, the latter as observed[19] also in the solid state and the former as found for the sterically more congested congener[22] **1b** (entry 1 in Table 1). This interpretation was corroborated by the numerical similarity of most of the secondary microsolvation criteria of **4** (entry 4) in comparisons with those of the two trisolvated test compounds (**2** and **3**) in entries 2 and 3: The practically equal upfield lithiation shifts $\Delta\delta = \delta(RLi) - \delta(RH)$ of C-4 or 4-H in entries 2–4 indicate comparable portions of electric charge to be delocalized from the carbanionic centers C-α into the α-aryl π systems. This energetically stabilizing, quasi-benzyl anion resonance[23] strives for maintaining a close to orthogonal orientation **7** of the α-aryl plane with respect to the $H_2C{=}C$ plane, so that the charge-bearing, quasi-sp^2 orbital at C-α can overlap with the p_z orbital at C-1 in the projection plane of **7**. The full set of $\Delta\delta$ data for monomeric **4**&3THF in THF is depicted in Figure S8a (Supporting Information)[21] for comparisons with those of the published[24] dimers, but it must be confessed that electric charges do not necessarily dominate the signs and magnitudes of $\Delta\delta$ for nuclei that are less remote from C-α than C-4 and 4-H. Of course, the possible suitability of $\Delta\delta$ as a secondary criterion does not hinge on our (in)ability to explain their observed values. On the other hand, the signs and magnitudes of the geminal olefinic two-bond coupling constants $^{2}J_{H,H}$ are less difficult to understand: As derived theoretically[25] and confirmed through correlation with inductive substituent constants,[26] $^{2}J_{H,H}$ values depend on electron-donating/-withdrawing substituent effects that are transmitted through the σ bonds in terminal olefins. Thus, the strongly positive value of $^{2}J_{H,H}$ = ca. 8.8 Hz in entries 2–4 of Table 1 indicates strong σ-donation from the $C{-}Li(THF)_3$ moieties, whereas the $C{-}Li(Et_2O)_2$ part in a disolvated

DOI: 10.1021/acs.joc.5b00762
J. Org. Chem. 2015, 80, 6313–6322

Table 1. Microsolvation Numbers *d* and NMR Data of α-(2-/6-Dimethylphenyl)vinyllithium (4) and Related 1b, 2, and 3 in Various Solvents[a]

									lithiation shifts Δδ [ppm]							
entry	cpd no.	2,6-substituent	solvent	equiv of donor	agg[b]	*d*	$^1J_{C,Li}$ [Hz]	$^2J_{H,H}$ [Hz][c]	C-α	C-β	β-H[d]	C-1	C-4	4-H	°C[e]	ref
1	**1b**	Me_2	THF[f]	THF	M	3	t, 10.7		+66.0	−17.3		+21.0	−12.4	−0.88	−95	22
2	**2**	*tert*-Bu_2	THF	THF	M	3	t, 10.8	8.5	+73.1	−7.2	−0.15	+23.5	−10.4	−0.78	−45	12
3	**3**	*i*-Pr_2	THF	THF	M	3	t, 11.0	9.0	+74.9	−8.6	−0.27	+24.0	−10.7	−0.78	−71	13
4	**4**	Me_2	THF	THF	M	3	t, 11.6	8.8	+76.4	−10.9	−0.43	+24.2	−11.0	−0.76	−89	g
5	**4**	Me_2	Et_2O	11 THF	M	3	t, 11.5	8.7	+75.6	−10.5	−0.42	+24.3	−10.9		−85	g
6	**4**	Me_2	*t*-BuOMe	3.3 THF	M	3	t, 11.7	8.5	+76.0	−10.7	−0.29	+24.5	−10.7		−87	g
7	**4**	Me_2	toluene	5.4 THF	M	3	t, 11.6	8.8	+76.7	−9.9	+0.47[h]	+24.4	−9.9	−0.02[h]	−92	g
8	**4**	Me_2	toluene	2.6 THF	M	3	t, 11.6	8.8	+76.6	−9.8	+0.51[h]	+24.4	−10.1		−102	g
9	**2**	*tert*-Bu_2	Et_2O	Et_2O	M	2	t, 13.7	7.4	+68.9	−7.3	−0.11	+22.0	−10.0	−0.71	−85	12
10	**3**	*i*-Pr_2	Et_2O	Et_2O	M	(i)	t, ≈12[i]	8.5[i]	+71.3	−6.0	−0.14	+23.1	−9.6	−0.58	−80	13
11	**3**	*i*-Pr_2	Et_2O	Et_2O	D	1	qi, 7.5	5.4	+66.9	−2.7	+0.16	+18.2	−6.5	−0.36	−80	13
12	**3**	*i*-Pr_2	*t*-BuOMe[j]	*t*-BuOMe	D	1	qi, 7.5	5.7	+66.2	−4.4	+0.16	+18.8	−6.8	−0.35	−69	13
13	**3**	*i*-Pr_2	C_5H_{10}[k]	≈1 *t*-BuOMe	D	1	qi, 7.7	5.0	+66.9	−3.9	+0.21	+18.5	−6.5	−0.31	−71	13
14	**4**	Me_2	*t*-BuOMe	3.3 THF	D	(1)			+70.7	−2.5					−87	g
15	**4**	Me_2	toluene	2.6 THF	D	1	qi, 6.8	6.7	+70.7	−2.4	+0.55[h]	+20.8	−7.2		−88	g
16	**4**	Me_2	toluene	5.4 THF	D	(1)		ca. 6.5	+70.7	−2.6	+0.54[h]	+20.8	−7.2	−0.02[h]	−92	g
17	**4**	Me_2	Et_2O	Et_2O	D	(1)		6.0	+69.1	−3.0	+0.11	+19.7	−7.0	−0.44	−58	19
18	**4**	Me_2	*t*-BuOMe	*t*-BuOMe	D	(1)		5.7	+68.1	−3.6	+0.13	+19.4	−7.0	−0.43	−40	19
19	**4**	Me_2	toluene	1.3 *t*-BuOMe	D	1	qi, 7.5	5.8	+68.2	−3.6	+0.64[h]	+19.6	−6.5	−0.02[h]	−84	19
20	**4**	Me_2	C_5H_{10}[k,l]	none	>D	0		3.8[n]	+57.4	+6.3	+0.26	+15.5	−3.5	−0.19	−35	g
21	**4**	Me_2	C_5H_{10}[k,m]	none	>D	0		4.0[n]	+58.7	+5.1	+0.21	+15.3	−3.6		−32	g

[a] *t* = triplet, qi = quintet. [b] "M" = monomer, "D" = dimer. [c] $^2J_{H,H}$ = 2.4(1) Hz for the parent olefin **9** in all four solvents. [d] β-H trans to α-aryl. [e] Temperature of determination of $\Delta\delta = \delta(RLi) - \delta(RH)$ [ppm]. [f] Table 1 of ref 22. [g] This work. [h] Temperature-dependent. [i] *d* = 3 and 2 (ca. 7:3) at −107 °C. [j] Microsolvation by *t*-BuOMe (1 equiv) detected at ≤ −69 °C. [k] C_5H_{10} = cyclopentane. [l] From iodoalkene **13**. [m] From dialkenylmercury **12** and with *n*-BuLi (0.4 equiv). [n] At +25 °C.

DOI: 10.1021/acs.joc.5b00762
J. Org. Chem. 2015, 80, 6313−6322

monomer ($^2J_{H,H}$ = 7.4 Hz in entry 9) is a weaker σ-electron donor. Accordingly, the value of $^2J_{H,H}$ = 8.5 Hz in entry 10 may be understood to be a weighted (7:3) average of 9 Hz (entry 3) and 7.4 Hz (entry 9) due to the alleged[13] rapid interconversion of tri- and disolvated monomers of **3**. A still weaker σ-donation from the $CLi_2(Don)_2$ moieties in the disolvated dimers (d = 1 donor ligand per Li) of **3** and **4** appears to account for $^2J_{H,H}$ = ca. 5.6 Hz in entries 11−13 and 19 and will be discussed in Section B; an independent effect of the decreased π-charge delocalization can be read from the $\Delta\delta$(C-4) values of ca. −6.6 ppm in those entries. The similarities of $^2J_{H,H}$ and/or $\Delta\delta$(C-α, C-β, C-1, and C-4) in entries 11−13 and 19 extend to the previously[19] described solutions of **4** in Et_2O (entry 17) or in *t*-BuOMe (entry 18) which did not provide $^1J_{C,Li}$ splitting of the ^{13}C-α signal for reasons of low solubility, so that neither aggregation nor microsolvation could be assessed. Relying on these secondary criteria ($^2J_{H,H}$ and $\Delta\delta$), however, we can now more confidently accept the disolvated dimers (**4**&Et_2O)$_2$ and (**4**&*t*-BuOMe)$_2$ to be the only species in those two solutions. With this information, it will become possible in Section C to rationalize a peculiar difference in the short-distance interactions that were detected by the method of heteronuclear (^{6}Li,^{1}H) Overhauser effect spectroscopy (HOESY) as follows. In Et_2O or *t*-BuOMe as the solvents, dimeric **4** exhibited HOESY cross-peaks[19] of ^{6}Li with the donor ligands Et_2O (CH_3 only)[27] or *t*-BuOMe (*t*-Bu and methyl protons), the 2,6-dimethyl hydrogens, and the vicinal olefinic trans-H (namely, cis to Li) at rt (room temperature). All these were also observed for monomeric **4**&3THF in THF at rt, except for the cross-peak of trans-H. We mention in passing that the related α-mesitylvinyllithium, **5**&3THF, was recognized to be a trisolvated monomer by its magnitude of $^1J_{C,Li}$ = 11.4(2) Hz in a ^{13}C-α triplet (1:1:1) at −113 °C in THF solution.[21]

Most of the ^{1}H and ^{13}C NMR chemical shifts δ of **4** in the above three ethereal solvents (Tables[21] S3−S5, Supporting Information) and also in toluene with *t*-BuOMe (1.3 equiv, Table[21] S6, Supporting Information) were practically independent of the temperature. As usual, this means that the dissolved single species maintained its aggegational state and degree of microsolvation at all investigated temperatures.[28] In the presence of lower THF concentrations, however, the chemical shifts of **4** were conspicuously temperature-dependent in Et_2O, *t*-BuOMe, or toluene as the solvents (Tables[21] S7−S14, Supporting Information). Clearly, each of the latter solutions contained more than one species of **4** in mobile equilibria whose components became evident at sufficiently low temperatures, where their mutual interconversion rates slowed down to below the regime of NMR time scales. By means of the primary criterion of $^1J_{C,Li}$ = 11.5−11.7 Hz with triplet splitting, the same trisolvated monomer **4**&3THF as in THF (entry 4 of Table 1) was recognized in Et_2O (entry 5, Table[21] S7), *t*-BuOMe (entry 6, Table[21] S9), and toluene (entry 7, Tables[21] S11−S13, Supporting Information). This was confirmed by the close resemblance of the total $\Delta\delta$ sets in Figures[21] S8a (in THF) and S8b (THF in Et_2O), while the concentration of **4**&3THF in the latter Et_2O solution was so low (Table[21] S8, Supporting Information) that $^1J_{C,Li}$ could not be measured. Incidentally, Table 1 shows that $^1J_{C,Li}$ does not depend significantly on the kind of these solvents, ligands, or the 2,6-dialkyl substituents, unless the microsolvation numbers d are changed (entry 9). The other equilibrium component in toluene was identified as the disolvated dimer (**4**&THF)$_2$ by the primary criterion of ^{13}C-α splitting patterns: The major species (now the dimer in entry 15) displayed a 1:2:3:2:1 quintet with $^1J_{C,Li}$ = 6.8 Hz at −88 °C (Table[21] S13, Supporting Information), which formally corresponds to at least d = 1 THF per Li according to eq 1 (since L = 46). The same THF-solvated dimer was present in Et_2O (Table[21] S8) and in *t*-BuOMe (entry 14 of Table 1; Tables[21] S9 and S10, Supporting Information), judging from the same $\Delta\delta$(C-α) value of ca. 70.7 ppm as in toluene solution (entry 16). Obviously, this preferred microsolvation by even small THF concentrations (down to 0.33 M in Table[21] S8) at low temperatures prevented the previously[19] reported precipitation of dimeric **4** from solutions in Et_2O or *t*-BuOMe. In the noncoordinating solvent toluene, however, the small THF concentration of 0.54 M (≤1.3 equiv only, Table[21] S14, Supporting Information) caused δ(C-α) to fall below the typical value of dimeric **4**, which points to the emergence of a further species of **4** (to be described in Section B).

$$2\ \mathbf{4}\&3THF \rightleftarrows (\mathbf{4}\&THF)_2 + 4\ THF \qquad (2)$$

The above identifications of the equilibrium components and their microsolvation numbers provided an occasion for our first thermodynamic quantification of the dimerization of a β-*un*substituted vinyllithium (**4**) in toluene on the basis of eq 2. Pursuing the previously[8] described protocol, we measured populations y_M of the monomer and $1 - y_M$ of the accompanying dimer (all in units of the monomeric formula **4**) initially at low enough temperatures through integrations of various ^{13}C NMR signals at their separated δ_M and δ_D resonance positions, respectively. Above certain coalescence temperatures, which depend on the individual differences $\delta_M - \delta_D$ of mutually interconverting pairs of ^{13}C nuclei, δ_M and δ_D had to be extrapolated (Figure S9, Supporting Information)[21] into the regions of higher interconversion rates where only averaged chemical shifts δ_{ave} could be detected and provided complementary population analyses by way of $y_M = (\delta_{ave} - \delta_D)/(\delta_M - \delta_D)$. As documented in Table[21] S1 (Supporting Information), the various y_M values were translated[19] into equilibrium constants K_{MD} in terms of eq 2. Over a temperature range from −102 to +25 °C, these K_{MD} values yielded the dimerization enthalpy ΔH^0, the entropy ΔS^0, and free enthalpies ΔG^0 according to $\Delta G^0 = -RT \ln K_{MD} = \Delta H^0 - T\Delta S^0$. The results are compared in Table 2 with the corresponding thermodynamic parameters of THF-solvated **1a** which had been obtained[8] with the same microsolvation numbers d_M = 3 and d_D = 1 as for **4**. The positive enthalpies ΔH^0 reveal that both **1a** and **4** dimerize endothermically; this process is energetically less expensive for **4** than for the sterically more congested **1a**. On the other hand, the strongly positive entropies ΔS^0 favor dimerization, which produces five particles (eq 2: the dimer plus four liberated THF molecules)

Table 2. Thermodynamic Parameters[a] ΔH^0 (kcal mol^{-1}) and ΔS^0 (cal mol^{-1} K^{-1}) for the Dimerization of 1a&3THF and 4&3THF in [D_8]toluene

	ΔH^0	ΔS^0	low/high[b]
1a[c]	+8.8 (±0.6)	+34.1 (±2.2)	−94/+75
4[d,e]	+5.8 (±0.2)	+27.6 (±0.9)	−102/+25

[a]Defined per dimer (namely, two monomers). [b]Low and high temperature limits (°C) of the measurements. [c]Reference 8. [d]This work. [e]Free dimerization enthalpy ΔG^0(0 °C) = −1.77 (±0.05) kcal mol^{-1}.

DOI: 10.1021/acs.joc.5b00762
J. Org. Chem. 2015, 80, 6313−6322

from two trisolvated monomers of both **1a** and **4**. Dividing ΔS^0 = 27.6 cal mol^{-1} K^{-1} for **4** by the balance of three independent particles, we find an average entropy gain of 9.2 cal mol^{-1} K^{-1} per particle, in close agreement with the magnitude of ca. 10 cal mol^{-1} K^{-1} for the mobilization of moderately sized organic molecules (relative masses ca. 100−300) in melting crystals.[29,30] Table 2 permits predictions of free dimerization enthalpies (and hence theoretical K_{MD} and δ_{ave} values) at any temperature: With ΔG^0(0 °C) = −1.77 kcal mol^{-1}, **4** is significantly more inclined to dimerize than **1a** (ΔG^0 = −0.5 kcal mol^{-1} at 0 °C), both with THF in toluene as the solvent.

Corresponding quantifications of the dimerization equilibria of THF-solvated **4** in the above-mentioned solvents Et_2O or *t*-BuOMe were not obtained for the following reasons. Preferential trisolvation of **4** by THF in those donor solvents was ascertained only at very low temperatures (Tables[21] S7−S10, Supporting Information). Therefore, we cannot exclude the possibility that the large excess of Et_2O or *t*-BuOMe contributes to microsolvation at the higher temperatures and thus invalidates eq 2. Nevertheless, qualitative evidence of endothermic dimerization of **4** under whatever kind of microsolvation remained perceptible from the averaged chemical shifts (Tables[21] S7−S10, Supporting Information) which moved toward δ_D of the dimer's values with increasing temperatures in a similar way as those depicted in Figure[21] S9 (Supporting Information).

B. Donor-Free 4 and Correlation of $^2J_{H,H}$ with Microsolvation. The absence of any electron-pair donor molecules is prerequisite to studies of the properties of **4** with the microsolvation number d = 0. The pertaining synthetic problem of obtaining clean samples of **4** in hydrocarbon solvents was tackled by means of the two alternative syntheses depicted in Scheme 3. First, a solution of the unpurified dimer (**4**&*t*-BuOMe)$_2$ in *t*-BuOMe was prepared as usual (Section A)[19] from bromoalkene **6** with *n*-BuLi and quenched immediately with $HgBr_2$ (0.5 equiv only) to give the dialkenylmercury **12**. (The corresponding monoalkenylmercury bromide that arose with 1 equiv of $HgBr_2$ proved unsatisfactory for generating clean **4**.) The ensuing Hg/Li interchange

Scheme 3. Preparation and Derivatization of Donor-Free 4

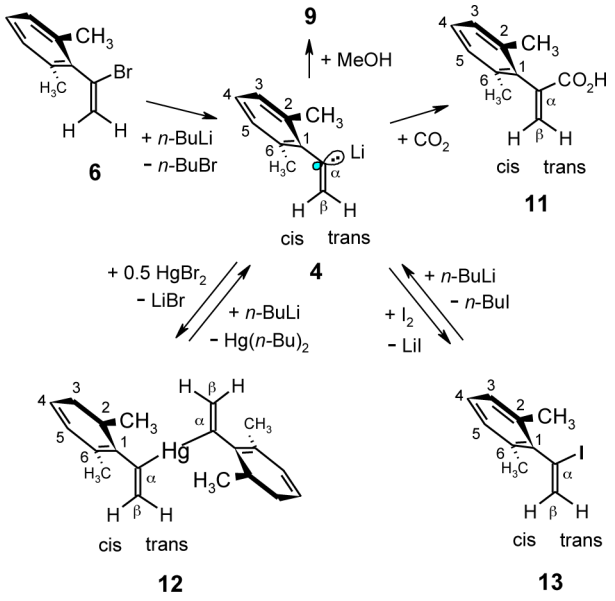

reaction of purified **12** with *t*-BuLi in pentane (4 h) or with *n*-Bu^{6}Li in cyclopentane (1 h) at rt led to partial precipitation of powdery **4**; nevertheless, the supernatants contained sufficient amounts of donor-free **4** for performing the NMR analyses: The desired geminal olefinic two-bond NMR coupling constant $^2J_{H,H}$ could be detected (4.0 Hz) only at rt because of severe line broadening of all proton signals on cooling down. Most of these and of the ^{13}C NMR signals separated into pairs of decoalesced signals at and below −32 °C, and all of them remained broad at lower temperatures. Therefore, the desired $^1J_{C,Li}$ couplings were never resolved, so that the two new species of **4** (intensity ratio 3:2) could not be identified. However, both of them are derived from **4** because quenching of these solutions with CO_2 or methanol produced the known[19] acid **11** or the parent olefin **9**, respectively. Thus, they must be higher aggregates since their δ values (Table[21] S15, Supporting Information) differ significantly from those of monomeric and dimeric **4**. In a search for better resolved spectra, we envisioned the following alternative synthesis.

The liquid iodoalkene **13** (Scheme 3) was obtained together with the olefin **9** from purified (**4**&*t*-BuOMe)$_2$ with elemental iodine. The ensuing I/Li interchange reaction of purified **13** with *n*-Bu^{6}Li in cyclopentane to give donor-free **4** was fast at rt (<10 min). The NMR analyses of such solutions could be extended over several hours, since the coproduct *n*-BuI did not react with both **4** and residual *n*-Bu^{6}Li. As above, the geminal coupling constant $^2J_{H,H}$ = 3.8 Hz was detected only at rt because of line broading, and $^1J_{C,Li}$ was again never observed at lower temperatures down to the solubility limits: In the absence of residual *n*-BuLi, the above NMR signal decoalescences did not take place (Table[21] S15, Supporting Information) down to −27 °C before **4** began to precipitate as a white powder. In the presence of *n*-BuLi, however, precipitation was delayed to below −66 °C, so that most of the ^{1}H and ^{13}C signals became decoalesced at and below −32 °C with formation of the same pairs of signals as observed above for the two species that had been generated from **12**. The relative intensities within these signal pairs varied with the concentrations of residual *n*-BuLi, which suggested that one of the two components of each pair belonged to some kind of a mixed, more soluble *n*-BuLi/**4** aggregate. Using the usually better solvent [D$_8$]toluene in addition to cyclopentane (4:1), we found once more $^2J_{H,H}$ = 3.8 Hz only at rt with line broadening and precipitation below −34 °C, so that again $^1J_{C,Li}$ splitting was not observed. Thus, the detailed structures of these two donor-free aggregates of **4** remained still unknown, but this did not impair the following analysis.

We note that practically equal values of $^2J_{H,H}$ = 3.9(1) Hz (entries 20 and 21 in Table 1) were obtained from the two above-mentioned, donor-free (d = 0) species of **4** irrespective of their ratios and their unknown structures (with and without *n*-BuLi), as testified by the four 25 °C entries in Table[21] S15b (Supporting Information). The reversed case of differing microsolvation yet unchanged monomeric constitution is shown in Table 1, where $^2J_{H,H}$ = 8.8(3) Hz for d = 3 in entries 2−8 changes to 7.4 Hz for d = 2 in entry 9; this certified that microsolvation alone may control $^2J_{H,H}$. Inclusion of the $^2J_{H,H}$ magnitudes of the disolvated dimers of **3** and **4** (d = 1 in entries 11, 12, and 17−19) led to the empirical eq 3, which assigns no explicit influence of aggregation on the d values. Figure 1 (line a) illustrates this linear increase of $^2J_{H,H}$ as a function of d = 0 (the aggregates), 1 (the dimers), and 2 and 3 (the monomers). However, why are we allowed to omit in eq 3 a direct influence

DOI: 10.1021/acs.joc.5b00762
J. Org. Chem. 2015, 80, 6313−6322

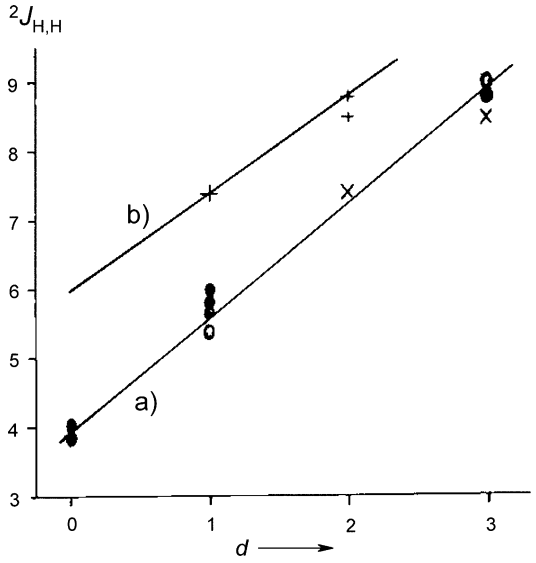

Figure 1. Dependence of the olefinic two-bond interproton coupling constants $^2J_{H,H}$ [Hz] on microsolvation numbers d (Table 1): Line a correlates **4** (filled symbols), **3** (open symbols), and **2** ("x"), while line b may have a slightly lower slope for dimeric and tetrameric $H_2C{=}CH{-}Li$[32] ("+") in THF.

of the varying numbers n of C−Li contacts in the monomers (n = 1), dimers (n = 2 as shown in Scheme 4), and higher

Scheme 4. One Olefinic Portion of the X-ray Structure[31] of the Dimer $(4\&Et_2O)_2$[a]

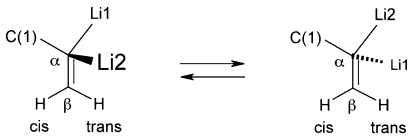

[a]Formula **14** shows Li2 above the projection plane that contains the approximate positions of Li1 and the other atoms, whereas **15** shows Li1 below the approximate plane of the other six atoms.

aggregates ($n \geq 2$)? The answer is based upon the known[25,26] dependence of $^2J_{H,H}$ on σ-inductive substituent effects (Section A) in combination with the insight that actually only one of two or three geminal $Li(Don)_d$ groups at C-α can exert this substituent effect fully through the olefinic σ-bonding framework. The latter statement may be verified through the following inspection of Scheme 4, which displays a relevant part of the X-ray structure[31] of the dimer $(4\&Et_2O)_2$.

$$^2J_{H,H} = 1.67d + 3.9\ [Hz] \quad (3)$$

C-α is situated almost within the C-β/C-1/Li1 plane, judging from the sum (357°) of the bond angles extending from C-α to C-β, C-1, and Li1 in **14**. Hence, Li1 maintains a σ-bonding relationship with the charge-carrying quasi-sp^2 orbital at C-α, whereas Li2 is above the projection plane of **14** with close to rectangular bond angles of C-β/C-α/Li2 = 81° and Li1/C-α/Li2 = 70°. With an angle of C-1/C-α/Li2 = 139°, Li2 is close to trans-H (distance 2.13 Å), in accord with the HOESY cross-peak of dimeric **4** (Section A) and its absence from monomeric **4** in which Li1 is too far apart from trans-H. Although all (four) C−Li bond distances have closely similar values (2.15−2.20 Å), $Li2(Don)_1$ is sufficiently above the projection plane so as to contribute much less than $Li1(Don)_1$ to the σ-bonding system that determines the signs and magnitudes of $^2J_{H,H}$. Of course, Li1 and Li2 will rapidly interchange their roles in a liquid phase through a slight rotational motion of C-1 and C-β about C-α with transformation of **14** into **15**, so that Li2 becomes the σ-bonding partner and Li1 moves to behind the projection plane; this fast process accounts for the increased apparent symmetry of the dimer as observed in the NMR spectra.

The above σ-bonding model and its consequences for $^2J_{H;H}$ apply also to unsubstituted vinyllithium: In terms of formula **14**, the X-ray structure[32] of the cube-type tetramer $(H_2C{=}CH{-}Li\&THF)_4$ revealed roughly planar domains with the σ-bonding Li1 at an angle of C-β/C-α/Li1 = 166°, whereas both Li2 and Li3 occupy almost rectangular positions (Li2/C-α/C-β and Li3/C-α/C-$\beta \approx 98°$)[32,33] even though all C−Li bond distances (2.24−2.26 Å) are practically equal. Thus, again only one of the three geminal $Li(THF)_1$ moieties at a certain C-α center is apt for efficient σ-bonding and hence decisive for $^2J_{H;H}$ = 7.4 Hz with d = 1 THF per Li in THF as the solvent.[34] Line b in Figure 1 suggests that the accompanying dimeric vinyllithium[34] with $^2J_{H;H}$ = 8.8 Hz (or 8.5 Hz with 1 equiv of TMEDA) in THF should be tetrasolvated (d = 2 rather than d = 1), in accord with the proposed[34] constitution, $(H_2C{=}CH{-}Li\&2THF)_2$. So far, all of these observations do not contradict the claim made in the empirical eq 3 that the degree of aggregation does not directly control the signs and magnitudes of the olefinic two-bond couplings $^2J_{H,H}$.

C. Differing sp^2-Stereoinversion Mechanisms. The direct preparation of donor-free **4** from bromoalkene **6** with a roughly equivalent amount of *n*-BuLi in pentane or toluene as the solvents was possible but preparatively unsatisfactory: The Br/Li interchange reaction was strongly retarded (requiring at least 22 h at rt for completion) and had to compete with the ensuing slow α-butylation of **4** by its coproduct *n*-BuBr to give **8**. This butylation could be outrun by an accelerated Br/Li interchange in the presence of a large excess of *n*-BuLi. In this manner, a sample of the known[35] 3:1 mixture of the deuteriated bromoalkenes (*E*)- and (*Z*)-[β-D_1]**6** (Scheme 5) was transformed into a mixture of (*Z*)- and (*E*)-[β-D_1]**4**, respectively, whose initially (within 1 min) observed molar ratio of ca. 2:1 supported the ^1H NMR assignments of the olefinic quasi-singlets, confirming that δ_H = 5.87 ppm belongs to the trans-H of (*Z*)-[β-D_1]**4** and 5.90 ppm to the cis-H of the (*E*)-isomer in hexane as the solvent. Within the next 5 min, this ratio changed

Scheme 5. Formation and Cis/Trans Diastereoisomerization of Donor-Free [β-D_1]4 in Hydrocarbons as the Solvent

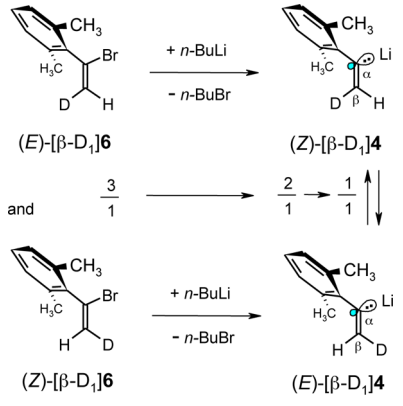

DOI: 10.1021/acs.joc.5b00762
J. Org. Chem. 2015, 80, 6313−6322

Table 3. Pseudoactivation Parameters $\Delta G_{\psi}^{\ddagger}$ (kcal mol^{-1} at 0 °C), $\Delta H_{\psi}^{\ddagger}$ (kcal mol^{-1}), and $\Delta S_{\psi}^{\ddagger}$ (cal mol^{-1} K^{-1}) of the Cis/Trans Diastereotopomerization Rates of Four Monomeric 1-(2,6-Dialkylphenyl)-1-alkenyllithiums (1−4) in THF (Entries 1−5), Compared with the Activation Parameters of Dimeric (4&*t*-BuOMe)$_2$ in Toluene (Entry 6)

entry	compound	aryl substituent	agg[a]	$\Delta G_{\psi}^{\ddagger}$ (0 °C)	$\Delta H_{\psi}^{\ddagger}$	$\Delta S_{\psi}^{\ddagger}$	reference
1	**1b**&3THF	2-/6-CH_3	M	12.47 ± 0.01	6.77 ± 0.18	−20.8 ± 0.7	22
2	**2**&3THF	2-/6-C$(CH_3)_3$	M	13.87 ± 0.01	7.02 ± 0.09	−25.1 ± 0.4	12
3	**3**&3THF	2-/6-CH$(CH_3)_2$	M	15.79 ± 0.07	9.3 ± 0.4	−23.6 ± 1.2	13
4	**4**&3THF	2-/6-CH_3	M[b]	16.3 ± 0.1	10.2 ± 0.7	−22.2 ± 2.2	this work
5	[β-D_1]**4**&3THF	2-/6-CH_3	M[c]	15.14 ± 0.01	8.79 ± 0.07	−23.3 ± 0.3	this work
6	(4&*t*-BuOMe)$_2$	2-/6-CH_3	D[d]	20.6 ± 0.5	20.8 ± 2.3	0.5 ± 5.8	19

[a]"M" = monomer, "D" = dimer. [b]Without LiBr. [c]With ca. 0.5 M LiBr (≈1 equiv). [d]In [D_8]toluene.

Scheme 6. THF-Catalyzed Ionization of Ground-State 16(CIP) Generates the Solvent-Separated Ion Pair 17(SSIP) and Is Followed by sp^2-Stereoinversion via a More Polar Transition State 18(SSIP) That Involves Migration of Li$^+$(THF)$_4$, Whereafter the Final Release of THF from 17′(SSIP) Forms the Cis/Trans-Inverted Ground-State 16′(CIP)

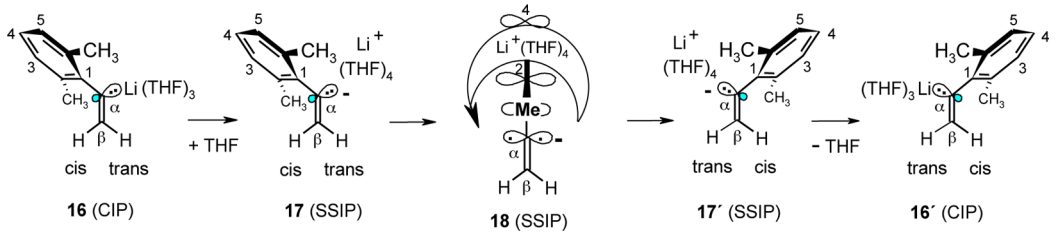

to 1:1, as expected for the equilibrium mixture, and remained so during further progress of the Br/Li interchange reaction and precipitation of LiBr. (The precise equilibrium ratio[21] was *E*/*Z* = 53:47 in both hexane and THF as the solvents.) This observation of the cis/trans isomerization of donor-free, aggregated **4** in hexane suggested a preinversion half-life time of roughly 1 min; ignoring the possibility of catalysis by the large excess of *n*-BuLi, this half-life translates into a free activation enthalpy of $\Delta G^{\ddagger}$(25 °C) = ca. 20 kcal mol^{-1}, to be compared with 20.6(5) kcal mol^{-1} as extrapolated from the previously[36] reported, analogous cis/trans diastereotopomerization of the disolvated dimer (**4**&*t*-BuOMe)$_2$ in toluene as the solvent. Since these two $\Delta G^{\ddagger}$ values are almost equal, we cannot exclude the possibility that both reactions take place by a similar mechanism. This process had been found[19] to occur with a kinetically first order of reaction and a vanishing entropy of activation (entry 6 in Table 3), which suggests that it proceeds within the disolvated dimer (without a dissociation) via an sp^2-stereoinversion mechanism that must be very different from that of monomeric **4** as described in the sequel.

The established[22] pseudomonomolecular, ionic sp^2-stereoinversion mechanism with strongly negative pseudoactivation entropies of monomeric, trisolvated α-arylalkenyllithiums[9,12,13,22] **1**−**3** in THF as the solvent (entries 1−3 of Table 3) applies also to monomeric **4** in THF: The trisolvated (Section A) ground-state contact ion pair (CIP) **16** in Scheme 6 starts through coordination of a fourth THF molecule with formation of the solvent-separated ion pair (SSIP) **17**. This immobilization of one THF particle accounts for part of the negative pseudoactivation entropies in entries 4 and 5. The enhanced charge separation in the intermediate **17** (SSIP) must be further increased in the transition state **18** (SSIP) so as to allow for migration of Li$^+$(THF)$_4$ (but without dissociation into the free ions). The present proposal of **18** is formulated in analogy with that of the paradigm case of **1a** and **1b** for which the full evidence had been reported.[22] The ensuing descent from **18** down to the inverted intermediate **17′** (SSIP) is followed by the final release of one THF ligand with formation of the cis/trans-inverted ground-state **16′** (CIP). Thus, the whole process is catalyzed by THF and hence "pseudomonomolecular" with the pseudoactivation parameters displayed in entries 4 and 5 of Table 3. As a consequence, the stereoinversion rates are always highest in THF as the solvent but substantially lower for the same THF-solvated monomers if THF is in short supply and converts **16** less efficiently into **17**. This mechanistic criterion was now found also for monomeric **4**&3THF with fast rates only in THF (Tables[21] S2a and S2b, Supporting Information) but not for **4**&3THF in Et_2O (Tables[21] S7 and S8), *t*-BuOMe (Tables[21] S9 and S10), or toluene (Tables[21] S11−S14).

Charge delocalization from C-α into the α-aryl group in the ground-state **16** of **4** implies a close to perpendicular conformation of the α-aryl ring plane with respect to the C-α/C-β double-bond plane (see **7** in Scheme 2) and creates a strong electronic resistance (ca. 12−15 kcal mol^{-1})[37] against rotation about the C-α/C-1 bond. This rotational barrier becomes even higher in the close to linear transition state **18** because the improved overlap of the coparallel p_z orbital axes at C-α and C-1 within the projection plane leads to an increased delocalization and energetic stabilization of the anionic charge in **18**. Clearly, a ca. 90° rotation about the C-α/C-1 bond into a coplanar α-aryl conformation would sacrifice this overlap together with its consequences. Hence, Li$^+$(THF)$_4$ will not be transported by the electronically impeded half-rotation of the α-aryl ring. On the other hand, migration across the unencumbered C-β region appears incompatible with the $\Delta G_{\psi}^{\ddagger}$ barriers of ca. 16 kcal mol^{-1} for stereoinversion of **4** (entries 4 and 5 of Table 3), which are much higher (rather than lower) than $\Delta G_{\psi}^{\ddagger}$ = 12.5 kcal mol^{-1} (entry 1) for **1b** despite its highly obstructed C-β region. Since Li$^+$(THF)$_4$ cannot be expected[22] to dissociate from the ion pairs **17** or **18**, it is thought to migrate along the charge gradients in the rotation-resistant α-aryl group and to surmount the aryl rim so as to arrive on the opposite aryl face. The alleged increase of charge separation on

DOI: 10.1021/acs.joc.5b00762
J. Org. Chem. 2015, 80, 6313−6322

the way from **16**(CIP) via **17**(SSIP) to **18**(SSIP) had been established[22] for **1a** and its *p*-substituted derivatives through a Hammett reaction constant of ρ = +5.2, which means that electron-donating substituents in the *p*-position of the α-aryl groups should retard the cis/trans interconversion rates. This mechanistic criterion was now met qualitatively with α-mesitylvinyllithium[21] (**5**&3THF), whose *p*-CH_3 substituent (σ_p^- = −0.17) lowered the rate to below the NMR time scale, so that its ^{1}H NMR spectrum displayed the expected two sharp olefinic AB-type doublets ($^2J_{H,H}$ = 8 Hz) up to 34 °C in THF as the solvent, whereas the corresponding AB-type spectrum of **4**&3THF in THF became broadened at rt and coalesced to give a singlet absorption at 72 °C; these clearly faster inversion rates of **4**&3THF confirmed the increasing charge separation during the ascent to **18**. Computer simulations[38] of the temperature-dependent line shapes in THF provided the pseudo-first-order cis/trans stereoinversion rate constants[21] k_ψ, whose temperature dependence (Figure 2, line a) had furnished the

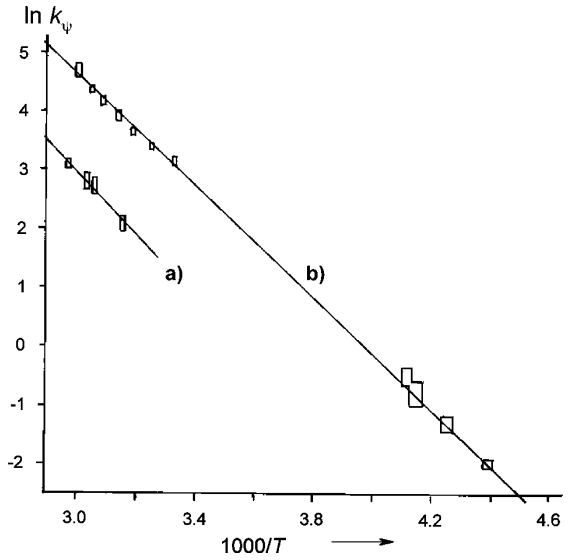

Figure 2. Arrhenius diagram showing how the natural logarithms (ln) of pseudo-first-order rate constants k_ψ [s^{-1}] of sp^2-stereoinversion in THF solution depend on 1000/*T* [K^{-1}] (a) for **4**&3THF in the absence of LiBr and (b) for [β-D_1]**4**&3THF with LiBr (ca. 1 equiv).

pseudoactivation data in entry 4 of Table 3. These line shapes (and their k_ψ values) remained unchanged by the following additions to the THF solutions: TMEDA, or *N*,*N*-bis(dimethylaminoethyl)aminomethane (PMDTA), or *p*,*p*′-di-*tert*-butylbiphenyl, the latter as a possible oxidant that might have formed a more rapidly inverting radical intermediate from **4**. On the other hand, in situ generated LiBr (a side-product in Scheme 3, up to 0.5 M, roughly 1 equiv) caused a modest (up to 6-fold) acceleration of the inversion process as depicted in line b of Figure 2 (Table[21] S2b, Supporting Information) for [β-D_1]**4** (for which the possibility of a kinetic isotope effect was excluded). With practically unchanged pseudoactivation entropies $\Delta S_\psi^\ddagger$ (entries 4 and 5), this acceleration is due to the lowered enthalpy $\Delta H_\psi^\ddagger$ in entry 5 versus 4. Since LiBr did not change the NMR data of the ground-state (**16**), this acceleration appears to point to an energetic stabilization of the transition state **18** due to an enhanced solvent polarity. As an alternative explanation, we mention a contest of the intramolecular $Li^+(THF)_4$ migration with a competing attack of external $Li^+(THF)_4$ Br^- on C-α from the opposite face of the α-aryl group in **18**; although this issue must be left open, it does not invalidate the ionic mechanism of Scheme 6. Aside from such LiBr effects, the enthalpic barriers $\Delta H_\psi^\ddagger$ increase with decreasing bulk of the 2-/6-substituents in entries 2−4 of Table 3, which may be ascribed to decreasing internal repulsions in the ground-states. A final comparison of the data in entries 1−5 with the strongly deviating activation parameters in entry 6 may serve to emphasize the different inversion mechanisms of the monomer **4**&3THF and the dimer (**4**&*t*-BuOMe)$_2$.

CONCLUSION

With the above investigation of the title compound **4**, we had left behind us the small regime of sterically congested alkenyllithiums (**3**, **2**, **1b**, **1a**, and some relatives[9,22] of **1a**), whose ("explicit") microsolvation by monodentate, ethereal (nonchelating) electron-pair donor ligands (and also by TMEDA in the case of **2**) could be measured directly through NMR integrations. Without shielding by the bulky β,β-di-*tert*-alkyl substituents in **1b**, however, the 2,6-dimethyl groups in **4** do no longer suffice to retard the rapid scrambling of coordinated and free donor ligands that prevents their differentiation. Instead, the microsolvation numbers *d* of **4** were obtained from the one-bond NMR coupling constants $^1J_{C,Li}$ via the empirical eq 1 [$d = L \times (n \times {}^1J_{C,Li})^{-1} - a$] that had been discovered previously[7] with **1a** and its congeners. Caused by this coupling, the splitting patterns of the ^{13}C-α NMR resonances gave primary NMR evidence of the monomeric or dimeric species of **4**. In addition, several lithiation shifts $\Delta\delta$ were confirmed to be suitable secondary criteria of aggregation and microsolvation. As a model compound, **4** appears to have been a fortunate choice because it formed three species with *d* = 0, 1, and 3. On combination of these with *d* = 2 Et_2O or *t*-BuOMe ligands[12] coordinating at monomeric **2**, the two-bond geminal coupling constants $^2J_{H,H}$ of the $H_2C{=}CLi$ parts emerged as a linear function of *d* in the new empirical eq 3. This convenient tool established $^2J_{H,H}$ as an auxiliary indicator of the microsolvation numbers, $d = ({}^2J_{H,H} - 3.9\ Hz) \times (1.67\ Hz)^{-1}$, of the present β-unsubstituted vinyllithiums and is based on the σ-electron-donating effects of $Li(Don)_d$ which grow in the sequence of *d* = 0 to 3. To be sure, this use of $^2J_{H,H}$ requires assisting evidence for the degree of (non)aggregation as available from $\Delta\delta$, $\delta(^{13}C\text{-}\alpha)$, or $^1J_{C,Li}$ (with the ^{13}C-α splitting patterns that provide *n* and *a* in eq 1), or otherwise; of course, these quantities should preferably be measured at a sufficiently low temperature so as to avoid obtaining an averaged value.

The trisolvation privilege of THF, as previously[22] formulated for **1a**, **1b**, **2**, and **3**, applies also to **4**: With *d* = 3, **4** is entirely monomeric in THF as the solvent but accompanied by the disolvated dimer (*d* = 1) if THF is in short supply. This endothermic dimerization furnished the third example[8] of a thermodynamic analysis that can yield correct entropy values with a proper allowance for the changing microsolvation numbers. Thus, microsolvation controls the aggregation modes of **4**: The C−$Li(THF)_3$ parts of two monomeric molecules of **4** are energetically lower by ca. 5.8 kcal mol^{-1} (Table 2) than the $C_2Li_2(THF)_2$ core of dimeric **4**, and the latter dimer is formed irreversibly from the donor-free aggregates of **4** on treatment with THF (or other donor ligands). Without THF, however, the disolvated dimeric species of **4** alone are tolerated in Et_2O or in *t*-BuOMe, whereas these solvents had previously[12] admitted merely *di*solvated monomers of α-(2,6-di-*tert*-butylphenyl)vinyllithium (**2**).

DOI: 10.1021/acs.joc.5b00762
J. Org. Chem. 2015, 80, 6313−6322

The kinetic privilege[22] of THF in cis/trans sp^2-stereoinversion is also based on the trisolvation of **4**: As for **1**−**3**, formation of the reactive SSIP intermediate **17** requires the transitory immobilization of only one further THF ligand on the way to the transition state (**18**) of the THF-catalyzed (hence pseudomonomolecular), ionic mechanism that is characterized by a strongly negative pseudoactivation entropy. Thus, microsolvation numbers control the rate of the pseudomonomolecular, ionic mechanism (monomeric **4**) and with it the degree of its kinetic preference over the corresponding (but mechanistically different) sp^2-stereoinversions of disolvated dimeric **4** (vanishing entropy of activation)[19] and of donor-free **4**, which were found to occur more slowly by factors of at least ca. 250 in hydrocarbon solutions at 25 °C.

EXPERIMENTAL SECTION

General Information. LiBr-containing samples of **4** or [β-D_1]**4** were obtained through Br/Li interchange reactions of **6** (or [β-D_1]**6**) with *n*-BuLi in pentane and did not crystallize; therefore, volatile contaminations were removed in vacuo, as specified in ref 13. The preparation and purification of LiBr-free **4** was described in ref 19, which provides additional details about dimeric **4**. Comments on the presentation and analyses of ^{1}H and ^{13}C NMR spectra may be found in ref 13. Rate measurements through ^{1}H NMR line shape analyses of the olefinic protons of **4** (coupled AB spectral system) were performed as reported[13,22] and were extended[21] to the uncoupled AB system of the two isotopomers of [β-D_1]**4**.

Monomeric α-(2,6-Dimethylphenyl)vinyllithium (4). The purified[19] dimer was dissolved in anhydrous THF. For ^{1}H NMR, see Table[21] S3b and Figures S1 and S3 (Supporting Information). ^{13}C NMR (THF, 100.6 MHz, +2 °C) δ 22.1 (qd, ^1J = 124.6 Hz, ^3J = 5.6 Hz, 2-/6-CH_3), 109.4 (dd, ^1J = 152.3 and 140.0 Hz, C-β), 116.5 (sharp d, ^1J = 154.9 Hz, C-4), 125.7 (narrow m, C-2/-6), 126.3 (dm, ^1J = 148 Hz, C-3/-5), 162.1 (unresolved, C-1), 212.0 (dd. ^2J = 13.0 and 8.5 Hz, C-α) ppm; compare Table[21] S3a and Figure S2 (Supporting Information).

Donor-Free 4 from 12. (a) *With t-BuLi*: A dry NMR tube (5 mm) was charged with the dialkenylmercury **12** (50 mg, 0.11 mmol) and pentane (0.5 mL). The suspension was cooled to −30 °C under argon gas cover and treated with *t*-BuLi (0.24 mmol) in pentane (0.16 mL). The total conversion of **12** to **4** required 4 h at rt and resulted in a slow precipitation of powdery, donor-free **4**. ^{1}H NMR: Table[21] S15b (Supporting Information). (b) *With n-BuLi*: The dialkenylmercury **12** (119 mg, 0.26 mmol) was placed in a dry NMR tube (5 mm), suspended in cyclopentane (0.7 mL), and cooled to −30 °C under argon gas cover for the addition of *n*-Bu^{6}Li (2.2 equiv) in cyclopentane (0.29 mL). After the total consumption of **12** within 60 min at rt, donor-free **4** precipitated slowly as above. ^{1}H NMR: Table[21] S15b (Supporting Information).

Donor-Free 4 from 13. A dry NMR tube (5 mm) was charged with the iodoalkene **13** (60 mg, 0.23 mmol) and either [D_8]toluene (0.5 mL) or cyclopentane (0.5 mL) with [D_{12}]cyclohexane (0.1 mL). After the addition of *n*-Bu^{6}Li (0.25 mmol) in cyclopentane (0.15 mL) at −30 °C under argon gas cover, **13** was entirely consumed within 10 min at rt. ^{1}H NMR: Table[21] S15b (Supporting Information). The coproduct *n*-BuI did not react with residual *n*-BuLi (if present) at rt.

Deuterium Isotope Effect on the *E*/*Z* Equilibrium of [β-D_1]4. The *E*/*Z* = 53:47 equilibrium ratio was found through ^{1}H NMR integrations of the two β-H quasi-singlets of [β-D_1]**4** in hexane as well as in [D_8]THF solution. Confirmations were obtained through deuteriolysis, which gave the "parent" olefins (*E*)- and (*Z*)-[α,β-D_2]**9** as follows. (a) [β-D_1]**4** in hexane was quenched with D_2O and worked up with Et_2O/H_2O to furnish the olefins [α,β-D_2]**9** (again *E*/*Z* = 53:47) as the only products. The cis-H of the *E* isomer was observed as a triplet ($^3J_{H,D}$ = 2.8 Hz) at δ_H = 5.20, the trans-H of the *Z* isomer as a triplet ($^3J_{H,D}$ = 1.8 Hz) at δ_H = 5.48 ppm in CCl_4. (b) [β-D_1]**4** in [D_8]THF was deuteriolyzed and measured in situ (−22 °C) at δ_H = 5.17 (0.55H) and 5.45 ppm (0.45H).

Bis[α-(2,6-dimethylphenyl)vinyl]mercury (12). A solution of the bromoalkene[19] **6** (150 mg, 0.71 mmol) in anhydrous *t*-BuOMe (1.0 mL) was cooled under argon gas cover to −30 °C, treated with *n*-BuLi (0.78 mmol) in hexane (0.62 mL), and warmed up to rt with soft swirling. The precipitating crystals of (**4**&*t*-BuOMe)$_2$ were redissolved at 30−40 °C, whereupon $HgBr_2$ (128 mg, 0.35 mmol) was added and formed a gray precipitate on further swirling for 30 min at rt. The mixture was diluted with dist. water (15 mL) and shaken with Et_2O (3 × 5 mL). The combined Et_2O extracts were washed with water (5 mL), dried over $MgSO_4$, filtered, and concentrated to leave the crude material (174 mg) that was recrystallized from EtOH: Yield 55 mg (33%) of pure **12** with mp 78−80 °C; ^{1}H NMR ($CDCl_3$, 400 MHz) δ 2.27 (s, 12H, 2 × 2-/6-CH_3), 5.36 and 5.56 (AB system, ^2J = 3.0 Hz, 2 × 2H, 2 × CH_2−β), 6.98 and 7.03 (AB_2 system, ^3J = 7.4 Hz, 2 + 4H, 4-H and 3-/5-H) ppm with a trace of the α-(arylvinyl)mercury bromide at δ 5.50 and 5.67 ppm; ^{13}C NMR ($CDCl_3$, 100.6 MHz) δ 21.2 (2 × 2-/6-CH_3), 125.5 (2 × C-4), 126.2 (^{199}Hg satellites, ^2J = 61 Hz; 2 × CH_2−β), 127.3 (2 × C-3/-5), 133.4 (2 × C-2/-6), 146.9 (2 × C-1), 181.6 (^{199}Hg satellites, ^1J = 1043 Hz; 2 × C-α) ppm, assigned through the characteristic ^{13}C,^{199}Hg NMR coupling constants of C-α and C-β, which leave straightforward assignments for the remaining one-carbon resonances (C-4 and C-1) and two-carbon signals (C-3/-5, C-2/-6, 2-/6-CH_3) by virtue of their δ regions of 120−129, 132−150, or ca. 20 ppm; IR (KBr) ν 3030, 2947, 2934, 2847, 1464 (s), 1065, 929 (s), 918 (s), 768 (s) cm^{-1}. The constitution was established through Hg/Li interchange reactions with *t*-BuLi (2.2 equiv) in pentane or *n*-BuLi (2.2 equiv) in cyclopentane to give solutions of donor-free **4**.

2,6-Dimethyl-α-iodostyrene (13). Purified dimer (**4**&*t*-BuOMe)$_2$ was prepared[19] from the bromoalkene **6** (400 mg, 1.89 mmol) and dissolved under argon gas cover in anhydrous Et_2O (3.0 mL), then cooled to 0 °C. After dropwise addition of a solution of elemental iodine (481 mg, 1.89 mmol) in anhydrous *t*-BuOMe (3.0 mL) and warm-up to rt for 30 min, the mixture was diluted with water (30 mL) and Et_2O (10 mL). The aqueous layer was shaken with Et_2O (3 × 10 mL), and the combined Et_2O phases were washed with aqueous $NaHSO_3$ (37%, 2 × 10 mL), washed with dist. water (10 mL), dried over $MgSO_4$, filtered, and concentrated to afford the crude iodoalkene **13** (179 mg). A distillation at 110−125 °C (bath temp.)/13 Torr under the strict exclusion of light yielded pure, liquid **13** (31% over two steps) after a forerun (17 mg) containing **13** and the olefin **9**. ^{1}H NMR ($CDCl_3$, 400 MHz) δ 2.30 (s, 6H, 2-/6-CH_3), 6.04 and 6.21 (AB system, ^2J= 1.2 Hz, 2H, 2 × β-H), 7.00 and 7.09 (A_2B system, ^3J = 7.5 Hz, 2 + 1H, 3-/5-H and 4-H) ppm; ^{13}C NMR ($CDCl_3$, 100.6 MHz) δ 19.9 (2-/6-CH_3), 104.0 (quart. C-α, calculated value 97.1), 127.6 (C-3/-5), 128.1 (C-4), 129.7 (CH_2−β, calculated value 126.4), 135.0 (quart. C-2/-6), 142.6 (quart. C-1) ppm, assigned through calculation of δ for C-α and C-β from the values reported[19] for the olefin **9** with the usual iodine increments of −38.1 and +7.0 ppm, respectively, which leaves straightforward assignments for the remaining one-carbon signals (C-4 and C-1) and two-carbon resonances (C-3/-5, C-2/-6, 2-/6-CH_3) by virtue of their δ regions (120−129, 132−150, or ca. 20 ppm); IR (film) ν 3063, 3018, 2950, 2918, 2851, 1624, 1465, 1377, 1190, 1051, 905, 770, 670, 575 cm^{-1}; MS (70 eV, 30 °C) *m*/*z* 258 (1%, M^+), 131 (87%, $M^+ - {}^{127}I$). Anal. Calcd for $C_{10}H_{11}I$ (258.10): C, 46.54; H, 4.30. Found: C, 47.27; H, 4.32.

ASSOCIATED CONTENT

Supporting Information

NMR spectra (Figures S1−S7), lithiation shifts (Figure S8), dimerization equilibrium (Figure S9, Table S1), cis/trans diastereotopomerization rate constants (Table S2), α-mesitylvinyllithium (**5**), and Tables S3−S15 of primary NMR data. The Supporting Information is available free of charge on the ACS Publications website at DOI: 10.1021/acs.joc.5b00762.

DOI: 10.1021/acs.joc.5b00762
J. Org. Chem. 2015, 80, 6313−6322

AUTHOR INFORMATION

Corresponding Author

*E-mail: rhk@cup.uni-muenchen.de (R.K.).

Notes

The authors declare no competing financial interest.

ACKNOWLEDGMENTS

This article is dedicated to Professor Dirk Trauner in recognition of his kind support. Financial support by the Deutsche Forschungsgemeinschaft during the earlier stages of this project is gratefully acknowledged.

REFERENCES

(1) Reich, H. J.; Kulicke, K. J. *J. Am. Chem. Soc.* **1996**, *118*, 273−274 and references quoted therein: Slow scrambling of the strong donor ligand $(Me_2N)_3PO$ ("HMPA").

(2) Henze, W.; Vyater, A.; Krause, N.; Gschwind, R. M. *J. Am. Chem. Soc.* **2005**, *127*, 17335−17342. Figure 8a (at 239 K) therein: Slow scrambling of THF at the endocyclic Li of dimeric $Me_2CuLi\&LiCN$.

(3) For intramolecular coordination by chelating donor functions, see: Fraenkel, G.; Cabral, J. A. *J. Am. Chem. Soc.* **1993**, *115*, 1551−1557.

(4) For an excellent contemporary collection, see: Reich, H. J. *Chem. Rev.* **2013**, *113*, 7130−7178.

(5) For a recent book on organolithiums and their aggregation/reactivity, see: Luisi, R., Capriati, V., Eds. *Lithium Compounds in Organic Synthesis: From Fundamentals to Applications*; Wiley-VCH: Weinheim, Germany, 2014.

(6) For a recent example of titration with the ligand THF in the noncoordinating solvent hexane, see: Liang, J.; Hoepker, A. C.; Bruneau, A. M.; Ma, Y.; Gupta, L.; Collum, D. B. *J. Org. Chem.* **2014**, *79*, 11885−11902. On page 11887 therein.

(7) Knorr, R.; Menke, T.; Ferchland, K.; Mehlstäubl, J.; Stephenson, D. S. *J. Am. Chem. Soc.* **2008**, *130*, 14179−14188.

(8) Knorr, R.; Menke, T.; Ferchland, K. *Organometallics* **2013**, *32*, 468−472.

(9) Knorr, R.; Hennig, K.-O.; Böhrer, P.; Schubert, B. *J. Organomet. Chem.* **2014**, *767*, 125−135.

(10) See Tables 2 and Supporting Information of ref 7.

(11) The usual equality of $n = a$ may be visualized from simplified presentations such as in ref 4 or in Chart 1 of ref 7.

(12) Knorr, R.; Knittl, M.; Rossmann, E. C. *Beilstein J. Org. Chem.* **2014**, *10*, 2521−2530.

(13) Knorr, R.; Ruhdorfer, J.; Böhrer, P. *Organometallics* **2015**, *34*, 1038−1045.

(14) Li, D.; Keresztes, I.; Hopson, R.; Williard, P. G. *Acc. Chem. Res.* **2009**, *42*, 270−280.

(15) With ^{13}C enrichment, for example: Su, C.; Hopson, R.; Williard, P. G. *J. Org. Chem.* **2013**, *78*, 11733−11746.

(16) Renny, J. S.; Tomasevich, L. L.; Tallmadge, E. V.; Collum, D. B. *Angew. Chem., Int. Ed.* **2013**, *52*, 11998−12013.

(17) Fraenkel, G.; Fraenkel, A. M.; Geckle, M. J.; Schloss, F. *J. Am. Chem. Soc.* **1979**, *101*, 4745−4747.

(18) von Roman, U.; Ruhdorfer, J.; Knorr, R. *Synthesis* **1993**, 985−992. Compound **11o** therein.

(19) Knorr, R.; Behringer, C.; Nöth, H.; Schmidt, M.; Lattke, E.; Räpple, E. *Chem. Ber./Recueil* **1997**, *130*, 585−592.

(20) See page 586 of ref 19.

(21) See the Supporting Information.

(22) Knorr, R.; Menke, T.; Behringer, C.; Ferchland, K.; Mehlstäubl, J.; Lattke, E. *Organometallics* **2013**, *32*, 4070−4081.

(23) For illustrations, see Section D of ref 22.

(24) Displayed in Figure 3 of ref 19.

(25) Pople, J. A.; Bothner-By, A. A. *J. Chem. Phys.* **1965**, *42*, 1339−1346.

(26) Knorr, R. *Tetrahedron* **1981**, *37*, 929−938. Figure 1 therein.

(27) See Figure 2 in ref 19.

(28) In contrast, monomeric **3** had been found[13] to be our first and hitherto only example with clear evidence for a partial desolvation and accompanying upfield NMR shifts on warming up.

(29) Page, M. I.; Jencks, W. P. *Proc. Natl. Acad. Sci. U.S.A.* **1971**, *68*, 1678−1683.

(30) Searle, M. S.; Williams, D. H. *J. Am. Chem. Soc.* **1992**, *114*, 10690−10697.

(31) See Figure 1 of ref 19.

(32) Bauer, W.; Hampel, F. *J. Chem. Soc., Chem. Commun.* **1992**, 903−905.

(33) Compare Figure 1b in ref 34 and the truncated formula **5** therein.

(34) Bauer, W.; Griesinger, C. *J. Am. Chem. Soc.* **1993**, *115*, 10871−10882.

(35) Compound $[D_1]$**10** on pages 585 and 591 of ref 19.

(36) See Section C of ref 19.

(37) See the experimental evidence outlined toward the end of Section A in ref 13.

(38) Binsch, G. *Top. Stereochem.* **1968**, *3*, 97−192. On pages 180−181 therein.

DOI: 10.1021/acs.joc.5b00762
J. Org. Chem. 2015, 80, 6313−6322